Deconstructing the *K*-band number counts

G. Barro[1], J. Gallego[1], P.G. Pérez-González[1], C. Eliche-Moral[1], M.Balcells[2], V.Villar[1], N.Cardiel[1], D. Cristobal-Hornillos[3], A.Gil de Paz[1], R. Gúzman[4], R. Pelló[5], M. Prieto[2] and J.Zamorano[1]

Abstract We present a study that links the NCs to the rest-frame luminosity functions (LFs) at the passbands probed by the observed K-band at different epochs. Making use of a large K-band selected sample in the Groth Field, HDFN and CDFS ($\sim$0.27deg^2), we have derived highly reliable photometric redshift estimates that allow us to estimate LFs in the redshift range [0.25-1.25]. We find that the larger flattening in the slope of the K-band NCs is mostly a consequence of a prominent decrease in the characteristic density (ϕ^*) around z$\sim$1, and an almost flat evolution of M^*.

1 Introduction

The galaxy number counts (NCs) are one of the most simple and yet useful consistency test to be performed on galaxy surveys. In particular, NIR galaxy counts have been traditionally considered a centerpiece of distant galaxy studies and a very useful method to constrain the models of galaxy evolution and cosmology. However, despite the apparent simplicity of the procedure, NCs represent sums of luminosity functions (LFs) modulated by shifts in apparent magnitude (due to the luminosity distance and the band redshift) and apparent number (due to to changes in the volume element and in the normalization of the LF). Thus, it is not surprising that, although the overall shape of the number counts is well defined, the full the interpretation in terms of the underlying galaxy populations still remains an open issue. Furthermore, there is a lack of agreement on the presence of some key features in the NCs such as a break in the slope of the K band number counts (K $\sim$17.5) [1, 2] or a roll over at very faint magnitudes. The origin of these controversies lies

(1) Universidad Complutense de Madrid (UCM), e-mail: gbc@astrax.fis.ucm.es · (2) Instituto de Astrofísica de Canarias (IAC) · (3) Instituto de Astrofísica de Andalucía (IAA) · (4) Universidad de Florida, USA · (5) Université de Toulouse, France

in the different observational bias affecting the galaxy surveys, that leads to a large scatter in the comparisons, lowering the chances to rule out some scenarios with statistical significance.

The purpose of the present study is to analyze the NCs in the K-band up to relatively bright magnitudes and provide a definitive understanding of the different parameters that drives the shape of the NCs, and particularly the presence of significant change in the slope around $K \sim 17.5$. Our approach to the problem takes advantage of all the power of the modern observational technology, combined with the break-troughs of photometric redshifts to dissect the relative contribution to the NCs from LFs at different redshift ranges.

2 The gears of the NCs

Here, we briefly outline the functional relation between the NCs and the LFs in the framework of a ΛCDM cosmology. Firstly, we assume that, in the full range of luminosities and redshift explored in this study, the galaxy LF can be represented in terms of a Schechter [3] function,

$$\phi(M) = 0.4\ln(10)\phi^* 10^{0.4(M^*-M)(\alpha+1)} \exp\left(10^{0.4(M^*-M)}\right) \quad (1)$$

where M^* is the characteristic absolute magnitude, α the faint-end slope, and ϕ^* the normalization of the luminosity function. In terms of this parametrization the expression for the NCs becomes,

$$\mathbf{N}(m_{\lambda_0}, [M,\phi,\alpha]_{\frac{\lambda_0}{(1+z)}}) = \int_{z_i}^{z_f} \phi(m, z, [M,\phi,\alpha]_{\frac{\lambda_0}{(1+z)}}) \frac{dV_c}{d\Omega} dz \quad (2)$$

where z_i and z_f are the lower and upper limit of the redshift bin, $dV_c/d\Omega$ is the differential comoving volume, and $m[M,\phi,\alpha]_{\frac{\lambda_0}{(1+z)}}$ represent the Schechter parameters of a LF in a band with effective wavelength $\frac{\lambda_0}{(1+z)}$. This term indicates the explicit dependence of the NCs on LFs at progressively shorter rest-frame wavelengths (e.g., the K-band probes the H-band at z$\sim$0.3, the J-band at z$\sim$0.7, etc.).

In the light of Eq. 1, NCs can be easily interpreted as a sum of LFs at different redshift bins, weighted by the corresponding comoving volumes. Hence, the shape of the NCs would be the result of the LF parameters at a given epoch and their evolution between redshifts, modulated by volume element. Straightforwardly, we can also summarize the evolution of the slope of the NCs in an schematic fashion. Attending to the most relevant features, we identify 3 main regimes:

- *The Euclidean regime.* The classic low redshift approximation to the slope of the NCs yields the well known result $d\log N/dm = 0.6$. The NCs in this regime are mostly populated by M$\leq M^*$ at z$\leq$ 0.2.
- *The transition regime.* It is dominated by the LF at the redshift that maximizes the product $\phi^*{}_{\frac{\lambda_0}{(1+z)}} \frac{dV_c}{d\Omega}$. In this regime the slope presents a significant decrement around the apparent magnitude of M^* at that redshift due to the knee in the LF. In absence of a significant evolution in ϕ^*, the maximum would take place at the peak of the volume element at z$\sim$2 (Bershady et al. 2003).
- *The α regime.* The main contributor in this regime are galaxies at the faint end of the LF. Therefore, the slope approaches asymptotically to -0.4(α+1). As a consequence of the previous regime, this phase would be dominated by the same LF as in the previous phase. However, other LFs not strongly suppressed by the $\phi^*{}_{\frac{\lambda_0}{(1+z)}} \frac{dV_c}{d\Omega}$ factor, having a significantly larger α, might take the lead of this phase.

3 *K*-band Number Counts and cosmic variance

In order to explore the nature of the K-band NCs, we have conducted a NIR survey at the 3.5m telescope of the Calar Alto Spanish-German Astronomical Center (CAHA), covering 2 separated fields centered at the Hubble Deep Field North and the Groth fields to a depth of $K \sim 19$. By combining our data with public deep K-band images in the CDFS (GOODS/ISAAC) and high quality imaging in multiple bands, we have extracted K-selected catalogs for a total of $\sim$14000 sources in a total combined area 0.27deg^2. Then, we have created a merged multi-wavelength catalog including all the optical and NIR bands available in the extensive coverage of these deep fields. Furthermore, we have characterized our sample with very accurate photometric ($\Delta z/(1+z) < 0.03$) redshifts based on a SED fitting procedure to empirical templates derived from stellar population synthesis models (see [4] for more details).

Based on the photometric redshift estimates, we have studied the relative contribution to the NCs in redshift bins ($\Delta z = 0.25$) within the range 0.25<z<1.25. Our results indicate that the contribution from low redshift galaxies (z<0.25) at $K > 15.5$ is almost insignificant (<10%), and that the majority of the counts below K< 18 come from galaxies at z<1 [5].

The left panel of Fig. 1 depicts the averaged NCs of the three fields along with counts from the literature. It can be seen that, although there is general consistency between the multiple measurements, the scatter is still large even at regions with low photometric errors. The most likely explanation for this differences is the cosmic variance. Taking advantage of our three pointings on different areas of the sky, we have been able to detect field to field differences that might reach the $\sim$40% between the most prominent LSS features. These

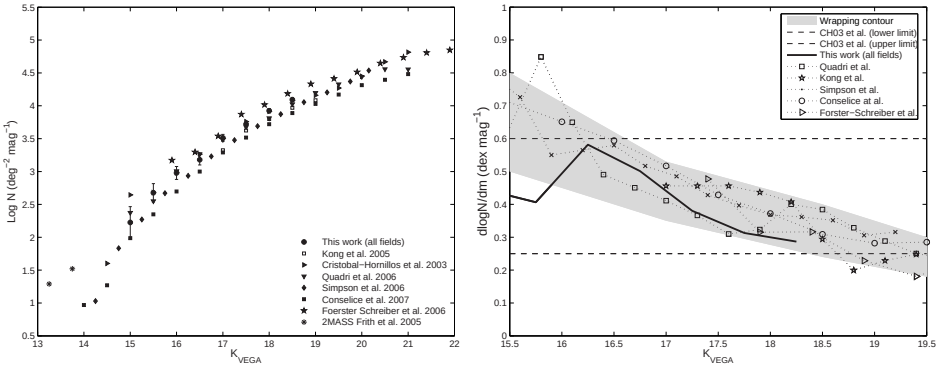

Fig. 1 *Left*: Averaged K-band number counts from Groth, HDFN and CDFS compared with a compilation of results taken from various sources. *Right*: Slope for the differential number counts in our three fields, along with data from the literature. The horizontal dashed lines indicates the value of the slope at both sides of $K = 17.5$ reported in [2].

variations are consistent with the amplitude of the discrepancies in the NCs. For instance, it can be seen that the NCs of [6] in the MS1054-03 galaxy cluster (z=0.83) present a prominent overdensity between 17< K <19. The right panel of Fig. 1 shows derivative of the NCs (i.e., the slope of the NCs). Again, the same significant fluctuations are present, but a general decreasing trend ($\sim$50% from $K = 16$ to $K = 18$) can be clearly identified. At this point, we conclude that substructure in the redshift distribution can cause significant fluctuations in the slope, that might lead to either a prominent break or a smoother decrement.

4 Number Counts from multi-band LFs

In order to disect the NCs in terms of more meaningful building blocks, related with the intrisical properties of the underlying galaxy population, we have calculated the LFs in four redshift bins: [0.25-0.50],[0.50-0.75],[0.75-1] and [1-1.25]. As we have already mentioned, the rest-frame bands probed by the observed K-band progressively shift towards shorter wavelengths. Therefore, to complement our estimates, we have compiled several LFs from the literature in optical [7, 8, 9] and NIR bands [10, 11, 12, 13] at different redshifts. By combining all these results, we have assembled a multi-λ, multi-redshift array that allow us to picture the evolutive pattern that gives rise to the K-band number counts. Since the NCs at relatively bright magnitudes are dominated by $z < 1$ galaxies, it is possible to recover the K-band NCs up to K< 19 just considering the contribution from a discrete number of LFs at low redshifts in a few bands. i.e the K-band at z=0, the H-band at

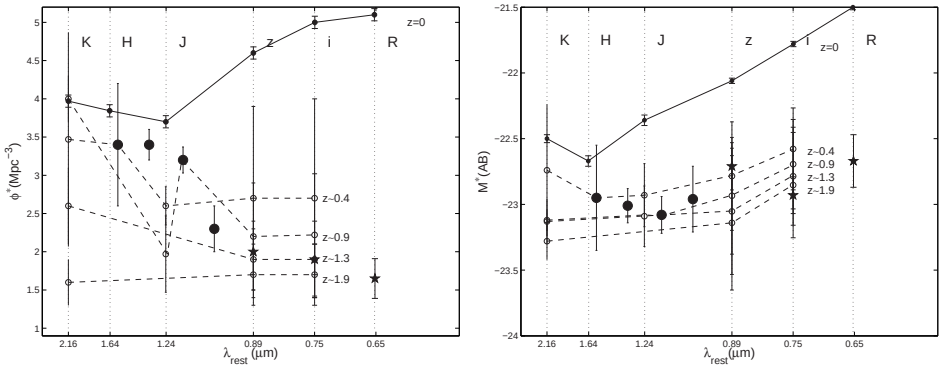

Fig. 2 Evolution with redshift of the Schechter parameters M^*(left panel), ϕ^*(right panel) in the $RizJK$ rest-frame bands. For each photometric band (RizJK, vertical dotted lines) the empty circles depict the redshift evolution of the parameter at $z \sim$ 0.4, 0.9, 1.3 and 1.9, drawn from different authors (see the text). The long dashed lines connect the values of the parameter at the same redshift in different bands. The black dots indicate the LF parameters at $\bar{z} = 0.38, 0.62, 0.88, 1.12$ derived in this work. The LFs as seen from the observed K-band probes the local K-band, then follow the black dots ($\sim H, J$) and finish with the black stars ($\sim$ z,i,R).

z$\sim$0.30, the J-band at z$\sim$0.70, etc. The two panels of Fig. 2 illustrate this idea showing the values of the Schechter parameters derived from our LFs along with other references in several bands and redshifts.

The analysis of the evolution in the Schechter parameters as probed by the observed K-band, reveals that the shape of the NCs is the byproduct of the almost constant values of the characteristic luminosity ($M^*_{K,obs}$; left panel of Fig. 2) and the progressive decline of the characteristic density ($\phi^*_{K,obs}$; right panel of Fig. 2). This decrement is especially significant around z$\sim$ 1, consistently with the results from other authors at higher redshifts [9, 14].

In the left panel of Fig. 3, we compare the predictions for the NCs derived from the array of LFs (Fig. 2) with the observational results shown in the left panel of Fig. 1 (the legend is the same). Not surprisingly, the predictions are quite similar to our NCs. More interestingly, the figure shows how the decrement in phi^* suppress the contribution from the z>1 bin (black stars) compared to the previous bin (small black dots), leading to a faster decrement in the slope of the NCs. In the right panel of Fig. 3 we show that expected slope in the case of no density evolution (black cross) produces an unrealistic larger slope. Similarly, a scenario with larger values of the faint end slope (α) at z> 0.5 leads to an equivalent result. In both cases the prediction is significantly out of the expectability regions for the observed NCs. Therefore, we can consistently argue that the dominant effect in the decrement of the slope around K$\sim$ 17.5 is a decrease in the characteristic density.

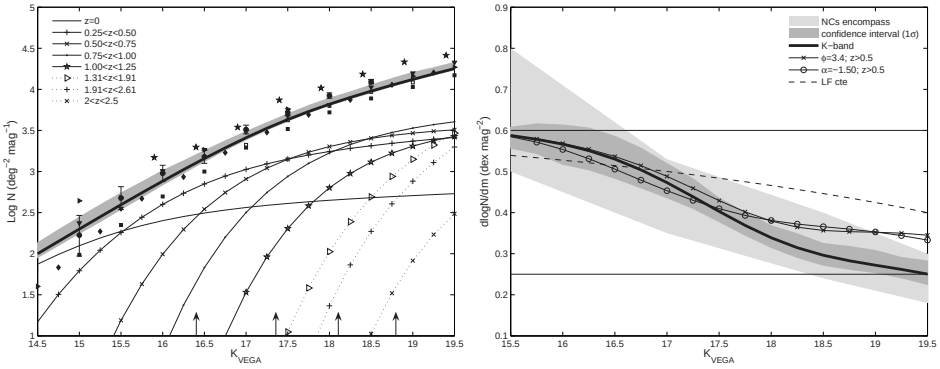

Fig. 3 *Left:* Predicted K-band NCs derived from the array of multi-band, multi-redshift LFs (Fig. 2) compared to data from other authors (the legend as in the left panel of Fig. 1). The shaded region indicates confidence interval derived from the uncertainties on the Schechter parameters. The continuous lines show the redshift binned number counts derived from our LFs. The dashed lines show the redshift binned NCs at higher redshifts from [9, 14]. The arrows depict the best-fit value of $M^*_{K,obs}$ for our LFs. *Right:* Slope of the predicted NCs (thick black line). The dark grey shaded region represents the same confidence interval as in the left panel. The light grey region encompass the slopes from the references. The circled and crossed lines show the predicted slope when fixing different Schechter parameters.

References

1. J.P. Gardner, L.L. Cowie, R.J. Wainscoat, ApJ **415**, L9 (1993). DOI 10.1086/187020
2. D. Cristóbal-Hornillos, M. Balcells, M. Prieto, et al., ApJ **595**, 71 (2003). DOI 10.1086/377215
3. P. Schechter, ApJ **203**, 297 (1976)
4. P.G. Pérez-González, G.H. Rieke, V. Villar, G. Barro, et al., ApJ **675**, 234 (2008). DOI 10.1086/523690
5. C.J. Conselice, K. Bundy, V. U, P. Eisenhardt, et al., MNRAS **383**, 1366 (2008). DOI 10.1111/j.1365-2966.2007.12686.x
6. N.M. Förster Schreiber, M. Franx, I. Labbé, et al., AJ **131**, 1891 (2006). DOI 10.1086/497293
7. M.R. Blanton, D.W. Hogg, N.A. Bahcall, J. Brinkmann, et al., ApJ **592**, 819 (2003). DOI 10.1086/375776
8. O. Ilbert, L. Tresse, E. Zucca, S. Bardelli, S. Arnouts, A&A **439**, 863 (2005). DOI 10.1051/0004-6361:20041961
9. A. Gabasch, U. Hopp, G. Feulner, R. Bender, S. Seitz, A&A **448**, 101 (2006). DOI 10.1051/0004-6361:20053986
10. S. Cole, P. Norberg, C.M. Baugh, C.S. Frenk, et al., MNRAS **326**, 255 (2001). DOI 10.1046/j.1365-8711.2001.04591.x
11. S. Arnouts, C.J. Walcher, O. Le Fevre, G. Zamorani, O. Ilbert, V. Le Brun, et al., ArXiv e-prints **705** (2007)
12. G. Feulner, R. Bender, N. Drory, U. Hopp, J. Snigula, G.J. Hill, MNRAS **342**, 605 (2003). DOI 10.1046/j.1365-8711.2003.06576.x
13. L. Pozzetti, A. Cimatti, G. Zamorani, E. Daddi, et al., A&A **402**, 837 (2003). DOI 10.1051/0004-6361:20030292

14. D. Marchesini, P. van Dokkum, et al., ApJ **656**, 42 (2007). DOI 10.1086/510305